First Computational Evidence of a Competitive Stepwise and Concerted Mechanism for the Reduction of Antimalarial Endoperoxides

Corinne Lacaze-Dufaure,*,† Fadia Najjar,‡,§ and Christiane André-Barrès‡

Centre Interuniversitaire de Recherche et d'Ingénierie des Matériaux, CNRS UMR 5085, ENSIACET, 4 allée Emile Monso, BP 44362, 31432 Toulouse cedex 04, France, Laboratoire de Synthèse et Physicochimie de Molécules d'Intérêt Biologique, CNRS UMR 5068, Université Paul Sabatier, 118 route de Narbonne, 31062 Toulouse, France, and Faculty of Sciences-2, Lebanese University, Jdaidet el-Maten, B.P. 90656, Lebanon

We study structural analogues of endoperoxides belonging to the family of G factors which present moderate to good antimalarial activity. Their biological activity is related to the reduction and cleavage of the O−O bond. Generally, the O−O bond reduction of model endoperoxides, as well as artemisinin, occurs by a concerted dissociative electron transfer (ET) mechanism. For the G3 and G3Me compounds, the experimental counterpart indicates an unexpected competition between a concerted and a stepwise mechanism, but no intermediate species can be isolated. We thus perform DFT studies on the reduction of G3 and G3Me compounds. We confirm the formation of an intermediate radical anion followed by cleavage of the O−O bond in a second step. We characterize the stable conformations for the radical anions $G_3^{\bullet -}$ and $G_3Me^{\bullet -}$ resulting from the ET and the associated reaction pathway. We also calculate the reorganization energy upon ET in relation to the Marcus theory using the DFT method. These results provide valuable insight into understanding the biological activity of G-factor endoperoxides as potential therapeutic antimalarial agents.

Artemisinin is a natural compound extracted from *Artemisia annua* L. (sweet wormwood). The molecule, presented in Figure 1, is currently used for its antimalarial properties. Other endoperoxides, called G factors, are extracted as such from the leaves of *Eucalyptus grandis* and other Myrtaceae. We have already reported the synthesis, antimalarial properties, and redox behavior of some G-factor derivatives (see Figure 2).[1−4] We have also previously looked for the most stable conformation of the G3 and G3Me molecules by DFT computations.[5]

The antimalarial activity of these compounds is related to the reduction of the O−O bond: the first step in the reduction mechanism of antimalarial endoperoxides is believed to be an electron transfer (ET) from heme iron[6−8] or free iron[9] to the O−O bond. For artemisinin, it results in the cleavage of the O−O bond, and the generated O-centered radicals rearrange to carbon-centered radicals and to alkylate heme or parasitic vital proteins.[6,7]

The reduction of artemisinin has been the purpose of many theoretical studies.[10−18] The O−O bond reduction of model endoperoxides, as well as artemisinin, was shown to occur by a concerted dissociative ET mechanism.[19−21] In the concerted mechanism, electron uptake by the peroxide and cleavage of the O−O bond are simultaneous (to within a bond vibration) to generate a spatially separated alkoxyl radical and an alkoxide, known as a distonic radical anion (see Scheme 1). In the stepwise mechanism, the initial ET results in the formation of an intermediate radical anion followed by cleavage of the O−O bond (k_{frag}) in a second step. Evidence for stepwise dissociative ET, and even the transition from concerted to stepwise ET, has been observed within a series of perbenzoates.[22,23] The overall

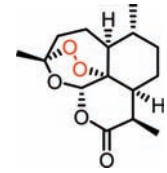

Figure 1. Artemisinin molecule.

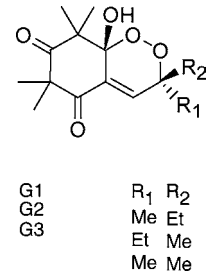

Figure 2. G-factors.

SCHEME 1: Stepwise and Concerted ET

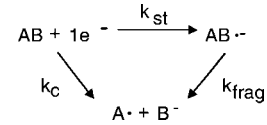

competition between the two mechanisms is dependent on various intrinsic properties of the reactive compound and even the reduction conditions. Thanks to cyclic voltammetry and convolution analysis, we proposed an unexpected competition between stepwise and concerted dissociative ET mechanisms for the heterogeneous reduction of the G factor endoperoxides G3 and G3Me.[4] This is the first time competition between these two mechanisms has been observed in endoperoxides. It implies the formation of an intermediate radical anion, not isolated

* To whom correspondence should be addressed. E-mail: corinne.dufaure@ensiacet.fr.
† ENSIACET.
‡ Université Paul Sabatier.
§ Lebanese University.

10.1021/jp100718p

experimentally, followed by cleavage of the O−O bond during the second step. Thus, we began a theoretical study of the dissociative ET reduction of the O−O bond in compound G3 and some derivatives to gain further mechanistic insights. Our aim was to investigate this reaction from an electrochemist's point of view.

In the present paper, we report theoretical studies of the G3 factor and its methylated derivative (G3Me). Our quantum studies focused on the determination of the stable conformations for the radical anions $G3^{\bullet -}$ and $G3Me^{\bullet -}$ resulting from the ET and on the localization of the transition state associated with the reaction pathway. We also calculated the reorganization energy upon ET in relation to the Marcus theory using the DFT method. All these results will contribute to a better understanding of the processes involved in the therapeutic action of G factors.

Theory and Methods

Marcus Theory. The original model reaction in Marcus theory is about the homogeneous transfer of an electron from a donor species, D, to an acceptor species, A:

$$D + A \rightleftarrows D^+ + A^-$$

The two systems of interest are the reactant state ($R = D + A$) and the product state ($P = D^+ + A^-$) and their intersecting diabatic free energy surfaces (with G* the minimum). The ET is a Franck−Condon process: the motion of the electron is instantaneous with regard to the motion of the nuclei. The passage of the electron from the donor to the acceptor can be effective if the donor and acceptor energy levels coincide. This implies a reorganization of the nuclei of the reactant to yield an appropriate configuration. Thus, the ET can be described in terms of potential energy surfaces as a function of a global nuclear coordinate, q.[24] The free energy of activation, $\Delta G^{\ddagger}$, for this reaction can be expressed as

$$\Delta G^{\ddagger} = \frac{(\lambda + \Delta G^{\circ})^2}{4\lambda}$$

with the driving thermodynamic force, $\Delta G^{\circ} = G_P^* - G_R^*$, and the reorganization energy, λ, of the system studied.

Marcus showed that λ can be divided into two terms: $\lambda = \lambda_{in} + \lambda_{out}$. λ_{in} is related to the molecular reorganization in the reactants, and λ_{out} is the contribution of the solvent surrounding the reactants to the reorganization energy. The term λ_{in} involves the energy of distorting the nuclear configuration while maintaining a particular electronic structure. It can be evaluated as the difference in the ab initio total energies from two calculations on the system, one for the equilibrium configuration (neutral state of the system) and one for the charge-transferred configuration. This is often called the direct method.[25,26] The term λ_{out} can be evaluated using several approaches. For instance, some model systems in the literature described DFT computations for a single active redox site (ion) with explicit solvent molecules for the first and second solvation shells in conjunction with a continuum model for the remaining solvent.[27] Molecular simulations also permit the calculation of λ_{out} including explicit solvent molecules.[28−31] Using a continuum model without taking into account explicit solvent molecules is another way to evaluate λ_{out}. We chose the Marcus continuum model.[32] This model is very simple, and the results are accurate enough for our study as we postulated that the solvent reorganization accompanying the reduction of the G3 molecules is not severe. This is consistent with the intramolecular reorganization of the G factors upon the ET. At a metal electrode, the Marcus formula for the calculation of λ_{out} is[33]

$$\lambda_{out} = \left(\frac{1}{D_{op}} - \frac{1}{D_s}\right)\frac{1}{4a}$$

with D_{op} and D_s the dynamic and static dielectric constants of the solvent, respectively, and a the hard-sphere radius of the species.

We are interested in the half-reaction: $O + e^- \rightarrow R$, where O and R indicate the oxidized and reduced species, namely, the G3 molecule and $G3^{\bullet -}$ radical anion. The above equation remains valid: the reactant state is composed of the oxidized species plus one free electron, and the product state is the reduced state.[29,30] This global system is thus in the oxidized or reduced state. To switch oxidation states, the system must find a surface crossing between the potential energy surface of the O and R states. The process takes place at one electrode, and it is thus a heterogeneous ET, but both reactant and product remain in solution. This simplifies the theoretical study of the process. The metal electrodes play the role of catalyst and have an influence on the kinetics but not on the thermodynamics of the process. The electrodes can be treated as a fictitious electron reservoir that behaves as a perfect electron donor.[29,30,34]

DFT Calculations. All structures were fully optimized using conjugate gradient methods with the Gaussian 03 software package.[35] We chose the B3LYP hybrid functional.[36,37] First, computations were done with the B3LYP/6-31G* scheme, and the stationary points were characterized as minima by a vibrational analysis. The zero-point energy (ZPE) corrections were taken into account. Starting from these structures, a new geometry optimization was carried out using the 6-311+G** basis set. Throughout all unrestricted calculations for the doublet state of the radical species, spin contamination was low with a value of $\langle S^2 \rangle$ of 0.76. The optimization step was followed by a Mulliken population analysis to have the charge and spin density on the atoms.

As we are looking for an intramolecular rearrangement following the electron transfer, we think that our computations in the gas phase will give significant details on the mechanisms of the ET. Nevertheless, computations in solution (CH_3CN) were performed for compound G3 and its radical anion in the framework of the polarizable dielectric model (SCRF-PCM). The optimized geometries and the resulting atomic spin densities were similar for the gas-phase and in-solution computations.

TABLE 1: Selected Calculated Bond Lengths for the G-Factors and the Artemisinin Molecule at the B3LYP/6-311+G Level of Theory**

molecule	O1−O2 (Å)	C4−C5 (Å)	C6−O7 (Å)
G3	1.458	1.337	1.216
G3Me	1.462	1.336	1.216
artemisinin	1.458		

Results and Discussion

Neutral Compounds: Geometry and Reactivity. We first present the results of our computations on the G3 factor and the methylated derivative (G3Me). For these molecules, the ground state is a singlet state. Some optimized bond lengths are given in Table 1. The only experimental data available are for the G1 factor. This compound has two different alkyl

TABLE 2: Total Energy (ZPE Included), Orbital Energies, and Reactivity Indices for the Neutral Molecules at the B3LYP/6-311+G Level of Theory**

	E_{tot} (au)	E_{LUMO} (eV)	$\Delta E_{HOMO/LUMO}$ ($\Delta E_{LUMO/LUMO+1}$) (eV)	η (eV)	ω (eV)
G3	−921.494963	−2.32	4.69 (1.22)	2.35	2.32
G3Me	−960.770609	−2.28	4.67 (1.28)	2.33	2.28
artemisinin	−960.773389	−0.45	6.75 (0.10)	3.37	1.08

functions (Me and Et) on C5, whereas the G3 factor has two Me functions on C5. We assumed that the O−O bond length should have close values in the two molecules. The calculated value of 1.458 Å (6-311+G**) thus compares well with the experimental counterpart of 1.479 Å for the G1 factor.[38] For the G3Me molecule, the O−O bond length is 1.462 Å. The C4−C5 bond length in the G3 and G3Me factors has a value of 1.336 Å, which is characteristic of a C═C double bond. The C−O bond length is 1.216 Å.

The value of 1.458 Å calculated for the O−O bond of the artemisinin molecule is in agreement with the geometrical parameter presented in the literature for the most stable conformation of artemisinin[17] and with the experimental value of 1.478 Å. In ref 17, the authors perform a conformational analysis of artemisinin by molecular dynamics and quantum chemistry calculations. They report seven stable conformers. Along the MD trajectories, one conformer (labeled atm2) represents 80% of all the probable conformers. The quantum calculations show that the atm2 conformer is the most stable one, and its simulated IR spectrum is in good agreement with experimental spectra. This is not the case for the other six conformers. This conformer is the one modeling with highest accuracy the experimental structure of artemisinin.

We found no significant differences between the optimized bond lengths for the in vacuo computations and the calculations in solution. This is in agreement with the study of Nosoongnoen and co-workers[17] on artemisinin.

The results of the gas-phase calculations in relation to the change in energy of the G factors upon an electronic transfer are reported in Table 2. The total energy including ZPE (E_{tot}) and the energies of the highest occupied molecular orbital (E_{HOMO}) and of the lowest unoccupied molecular orbital (E_{LUMO}) are given. We use some reactivity indices as described by Parr[39] and used by Moens et al.[34] In their study, the authors also focused on the properties of single molecules involved in reduction half-reactions. The chemical hardness η measures the stability of a system in terms of resistance to electron transfer.[39] It is calculated from the ionization potential, I, and the electron affinity, A, with the relation

$$\eta = \frac{I - A}{2}$$

The electrophilicity ω[40,41] measures the ability of a molecule to accept electrons from a perfect electron donor (a sea of electrons of zero chemical potential and zero hardness at 0 K). It is calculated with the relation

$$\omega = \frac{(I + A)^2}{8(I - A)}$$

We approximate the ionization potential and the electron affinity by the frontier orbital energies (Koopman's theorem assuming frozen orbitals):

$$E_{HOMO} = -I \quad \text{and} \quad E_{LUMO} = -A$$

The G3 and the G3Me factors exhibit the lowest energy for the LUMO, the smaller HOMO/LUMO gap, the lowest chemical hardness, and the highest electrophilicity. We can conclude that these molecules will accept electrons more easily from an ideal reservoir (electrode) than the artemisinin compound.

For the G3 molecule, the LUMO is shown in Figure 3. It presents a π^* character and is delocalized on the C6═O7 and C4═C5 bonds. The LUMO + 1 orbital is 1.22 eV higher in energy (6-311+G**) and is on the O1 and O2 atoms (σ^* character). A detailed investigation of the G3Me molecule comes to the same conclusion with the LUMO orbital of the π^* type and a LUMO/LUMO + 1 gap of 1.28 eV.

The LUMO and LUMO + 1 orbitals of the artemisinin molecule are presented in Figure 4. These orbitals are very close in energy as the LUMO/LUMO + 1 gap is 0.10 eV. The LUMO orbital is on the C═O group and has a π^* character. The LUMO + 1 orbital is mainly on the O−O bond and has a σ^* character.

Radicals. We are interested in the reduction of the antimalarial endoperoxides. We looked for the stable conformations of the radical anions coming from the reduction of the G3, G3Me, and artemisinin molecules. We present the results of the computations in vacuo. All the structures are presented in Figure 5, and the associated geometric and energetic parameters are in Tables 3 and 4.

For the $G3^{\bullet -}$ radical, we found two stable conformations named A and B. They are characteristic of a stepwise reduction mechanism. The possibility of a stepwise dissociative mechanism is described for some examples in the literature.[22] In the stepwise mechanism, the initial electronic transfer results in the formation of an intermediate radical anion followed by cleavage of the O−O bond in a second step (see Schemes 1 and 2).

If we compare the bond lengths of the C4═C5 and the C6═O7 bonds in the G3/G3Me molecules and in conformation A of the radical, we see that they are elongated. The other geometric parameters on the molecule are not significantly changed, and we note that the O−O bond length is unchanged.

When the G3 molecule gets an electron, it goes on the LUMO orbital (π^* character on C4═C5 and C6═O7). The spin densities on radical A show that the unpaired electron is delocalized on the C4═C5−C6═O7 group and the SOMO of conformation A is on these atoms. Conformation B is 1.38 eV (31.8 kcal/mol) lower in energy. It is the thermodynamic product. There is an extra electron on the α energy levels, and the associated orbital has a σ^* character on the O1−O2 bond. The spin densities show that the unpaired electron is located on this O1−O2 bond.

We investigated the reaction pathway between conformation A and conformation B. The transition state is situated respectively at 0.15 eV (3.46 kcal/mol) and 1.53 eV (35.28 kcal/mol) for conformation A and conformation B of the reduced G3 molecule. The process A → B is thus slightly endothermic. For the transition state, the unpaired electron is delocalized on the O1−O2 and C4═C5−C6═O7 groups of the molecule.

We found only one stable conformation for the radical anion associated with artemisinin. It was also reported in the literature.[11,12,16,18] This is in agreement with the reduction of artemisinin that takes place via a concerted dissociative ET mechanism. The neutral/anion energy gap is 1.68 eV (38.74 kcal/mol) (1.44 eV/B3LYP 6-31G* in the literature[16]). It is clear from the spin densities on the reduced compound that the unpaired electron is located on the O atoms of the broken endoperoxide bond. The LUMO/LUMO + 1 gap in the neutral compound is 0.10 eV, and the two orbitals are thus energetically

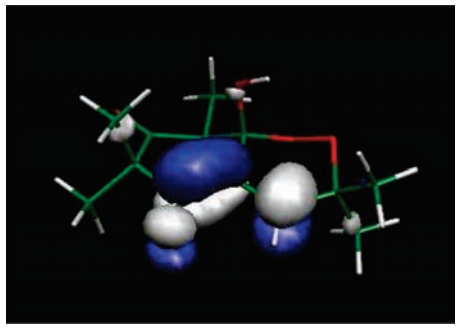

Figure 3. LUMO of the G3-factor.

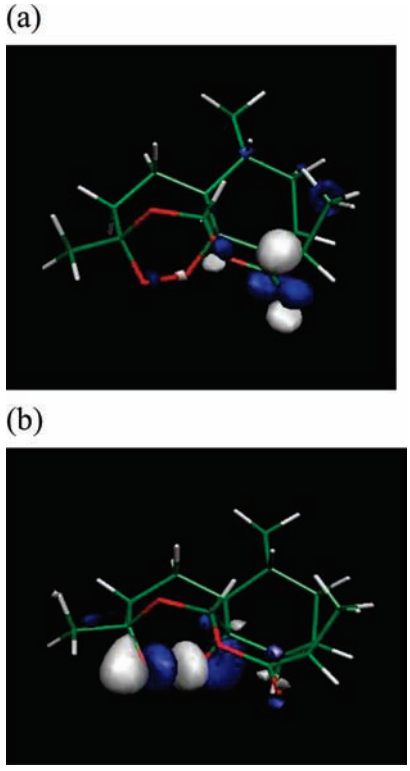

Figure 4. LUMO (a) and LUMO + 1 (b) of the artemisinin molecule.

accessible. The electron is accepted during the reduction process into the σ^* LUMO + 1 orbital, largely associated with the O−O bond. This results in a cleavage of the endoperoxide bond.

Calculation of the Reorganization Energy. We calculated the reorganization energy for the G factors and the artemisinin molecule. We used the four-point method described by Rosso et al.[26] depicted in Scheme 3. In this approach that is derived from the Marcus theory, the potential energy surfaces (PESs) of the reactant and of the product are approximated by harmonic curves. The minimum of the PESs of the reactant and of the product represents the optimized geometry for the oxidized and reduced compounds, respectively. The reorganization energy can be calculated in two ways: (i) on the PES of the reactant as the difference between the total energy of the compound in its optimized geometry and the total energy of the compound with a geometry corresponding to that of the optimized product (λ_r) or (ii) on the PES of the product as the difference between the total energy of the compound in its optimized geometry and the total energy of the compound with a geometry corresponding to that of the optimized reactant (λ_p). The reorganization energy is the free energy decrease on the same diabatic surface; thus, this quantity is independent of the driving thermodynamic force.

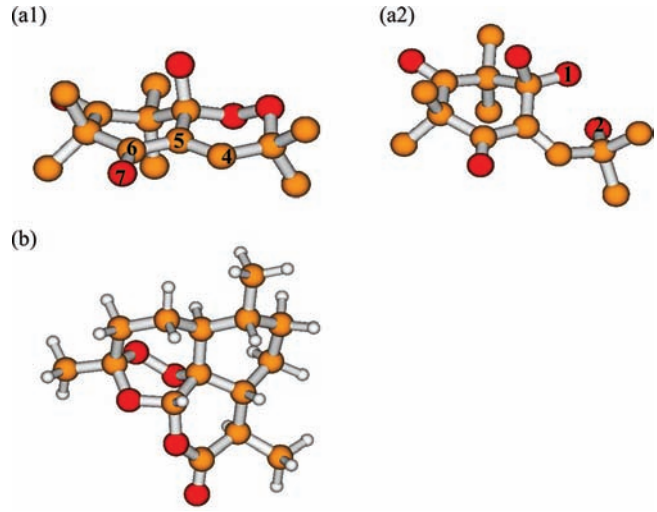

Figure 5. Radical compounds coming from the reduction of the G3 (a1, radical A; a2, radical B) and artemisinin (b) molecules.

TABLE 3: Relative Energy and Selected Calculated Bond Lengths for the Radical Anions at the B3LYP/6-311+G Level of Theory**

molecule	ΔE^a (eV)	O1−O2 (Å)	C4=C5 (Å)	C6=O7 (Å)
G3, radical A	1.06	1.455	1.397	1.265
G3, radical B	2.44	2.260	1.341	1.225
G3, transition state	0.91	1.601	1.384	1.258
G3Me, radical A	1.04	1.458	1.395	1.265
G3Me, radical B	2.34	2.243	1.343	1.225
artemisinin	1.81	2.202		
	1.44[b]	2.185[c]		

[a] $\Delta E = E_{tot}$ (neutral molecule) − E_{tot}(radical). E_{tot} includes ZPE corrections. [b] Reference 12. B3LYP/6-31G* results not including ZPE corrections. [c] References 16 and 17.

TABLE 4: Atomic Spin Densities on the Radical Anions at the B3LYP/6-311+G Level of Theory**

	O1	O2	C3	C4	C5	C6	O7
G3, radical A	0.00	0.00	−0.01	+0.62	−0.03	+0.20	+0.19
G3, radical B	+0.43	+0.51	−0.02	0.00	+0.03	0.00	0.00
G3, transition state	+0.08	+0.08	−0.02	+0.48	−0.01	+0.16	+0.15
G3Me, radical A	0.00	0.00	0.00	+0.63	−0.01	+0.19	+0.19
G3Me, radical B	+0.34	+0.58	−0.02	+0.02	+0.03	0.00	0.00
artemisinin	+0.23	+0.22					
	+0.51[a]	+0.45[a]					

[a] Reference 12. B3LYP/6-31G* results.

It is used to calculate the term λ_{in} as the average value: $\lambda_{in} = (\lambda_r + \lambda_p)/2$.

We calculate the thermodynamic driving force for the two processes: 22.0 and 53.7 kcal/mol for the G3 → radical A and G3 → radical B processes, respectively. Using the computational approach described above, we found for the G3 molecule a reorganization energy, λ_{in}, of 7.82 and 41.05 kcal/mol for G3 → radical A and G3 → radical B, respectively. For the first process (G3 → A), the geometrical parameters (Table 3) showed a small geometrical change upon the ET, and the reorganization energy is thus lower than for the G3 → B process where the electronic transfer is dissociative. With the continuum model, the λ_{out} term was evaluated at 0.52 kcal/mol.

We finally calculated the intrinsic activation energy, $\Delta G^{\circ\ddagger}$. It is the activation energy when the driving force is equal to zero: $\Delta G^{\circ\ddagger} = \lambda/4$. The intrinsic activation energy is lower for the G3 → A process with a value of 2.09 kcal/mol than for the G3 → B process with a value of 10.41 kcal/mol.

SCHEME 2: Reduction of the G3-Factors

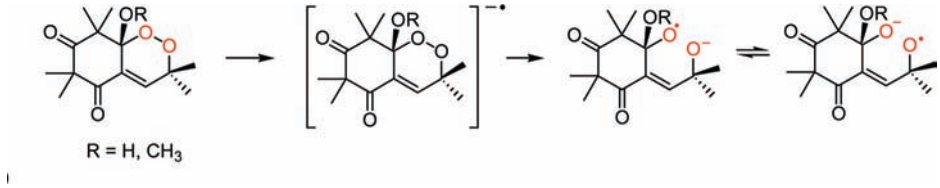

SCHEME 3: Potential Energy Diagrams for the Calculation of the Reorganization Energy with the Four-Point Method[26]

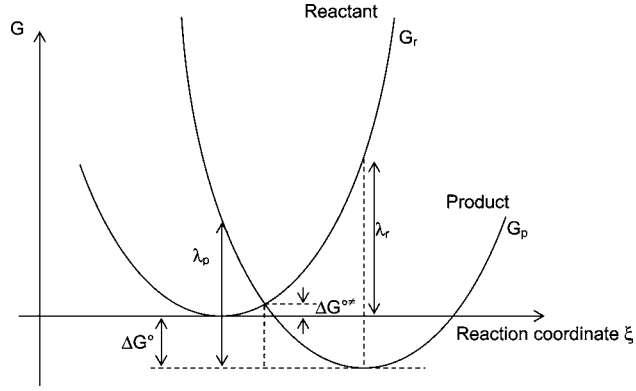

The theoretical values of the intrinsic barrier, $\Delta G^{\circ\ddagger}$, can be compared with experimental ones obtained previously using the convolution method for the treatment of voltammetry curves at different scan rates (Table 5)[4] and using the Savéant model.[42] According to this model, the intrinsic barrier (i.e., the activation energy at zero driving force) is a function of the bond dissociation energy (BDE) of the fragmenting bond and the reorganization energy, λ.

Therefore, for the concerted mechanism the intrinsic barrier is expressed as follows:

$$\Delta G_c^{\circ\ddagger} = \frac{\lambda_c + \mathrm{BDE}}{4}$$

where λ_c is the reorganization energy of the concerted mechanism. For the stepwise mechanism the expression is simplified as there is no contribution from the BDE:

$$\Delta G_{st}^{\circ\ddagger} = \frac{\lambda_{st}}{4}$$

where λ_{st} is the reorganization energy of the stepwise mechanism.

The convolution analysis allows determination of the heterogeneous electron transfer rate constant, k_{ET}, the activation energy, $\Delta G^{\ddagger}$, of the reaction, and the transfer coefficient, α, as a function of the potential along a cyclic voltammetry peak. k_{ET} is related to $\Delta G^{\ddagger}$ by an Eyring-type equation:

$$k_{ET} = Z \exp\left[-\frac{\Delta G^{\ddagger}}{RT}\right]$$

where Z is the Arrhenius preexponential factor including the electron transmission coefficient, κ.

The transfer coefficient (α) represents the dependence of the intrinsic barrier on the free energy, ΔG°:

$$\alpha = \frac{\partial \Delta G^{\ddagger}}{\partial \Delta G^{\circ}} = \frac{-RT}{F}\frac{\mathrm{d}\ln k_{ET}}{\mathrm{d}E}$$

A detailed analysis of α as a function of the potential revealed that both concerted and stepwise dissociative electron transfers occur at the same potential, so the observed k_{ET} is the sum of the individual rate contants k_c and k_{st} (concerted and stepwise mechanisms, respectively). The theoretical fits of α as a function of the potential, on the experimental ones by adjustment of the various parameters in a physically realistic range, allowed us to evaluate the parameters $\Delta G_c^{\circ\ddagger}$, $\Delta G_{st}^{\circ\ddagger}$, E_c°, E_{st}°, and Z_{st}/Z_c, which are summarized in Table 5.

The experimental values[4] are in the range of $\Delta G_{st}^{\circ\ddagger} \approx 1$ kcal/mol and $\Delta G_c^{\circ\ddagger} \approx 12$ kcal/mol, respectively, for the stepwise and concerted mechanisms. The theoretical values are in good agreement with the experimental ones.

For the artemisinin molecule, we calculated a thermodynamic driving force of 45.19 kcal/mol, a reorganization energy, λ_{in}, of 48.15 kcal/mol, and an intrinsic activation energy of 12.18 kcal/mol in agreement with the experimental value of 8−12 kcal/mol.[43]

Conclusion

To our knowledge, the present study constitutes a breakthrough in understanding the mechanism for the antimalarial mode of action of G-factors. On the basis of the results obtained, we draw the following conclusions.

(i) The two stable conformations for the radical anions associated with the G3 and the G3Me factors concern the stepwise mechanism proposed experimentally for the reduction of the G3 and G3Me molecules. We characterized the transition state between the two radicals.

(ii) For the artemisinin molecule, we found only one stable conformation for the reduced species. The concerted mechanism is confirmed.

(iii) We computed the reorganization energy and the intrinsic activation energy associated with the electronic transfer. The

TABLE 5: Thermodynamic Data for the Heterogeneous Reduction of Endoperoxides G3 and G3Me[a]

	Z_{st}/Z_c	$\Delta G_c^{\circ\ddagger}$ (kcal·mol^{-1})	$\Delta G_{st}^{\circ\ddagger}$ (kcal·mol^{-1})	λ_c (kcal·mol^{-1})	λ_{st} (kcal·mol^{-1})	E_c° (V)	E_{st}° (V)	BDE (kcal·mol^{-1})
G3	50	12.4	0.98	15.9	3.9	−0.82	−1.70	33.8
G3Me	50	11.7	1.1	15.5	4.4	−0.84	−1.64	31.4

[a] Z is the Arrhenius preexponential factor, $\Delta G^{\circ\ddagger}$ is the intrinsic activation energy, λ is the reorganization energy, E° is the standard potential, and BDE is the bond dissociation energy of the O−O bond. The subscripts c and st are for the concerted and the stepwise mechanisms, respectively.

calculated values are in good agreement with their available experimental counterparts and validate the computational approach.

(iv) The two stable forms for radical anions A and B of compound G3 can be attributed to the product of the stepwise and concerted mechanisms, respectively.

(v) Steric hindrance around the peroxide bond can be bypassed as the electron is first transferred to the π^* orbital of the conjugated double bond when the stepwise mechanism is observed.

Acknowledgment. We thank CALMIP (CALcul intensif en MIdi Pyrénées) and the CICT (Centre Interuniversitaire de Calcul de Toulouse) for providing computer time on the supercomputer Soleil and AUF (Agence Universitaire de Francophonie) for a grant to F.N.

References and Notes

(1) Najjar, F.; Baltas, M.; Gorrichon, L.; Moreno, Y.; Tzedakis, T.; Vial, H.; André-Barrès, C. *Eur. J. Org. Chem.* **2003**, *17*, 3335–3343.

(2) André-Barrès, C.; Najjar, F.; Bottalla, A.-L.; Massou, S.; Zedde, C.; Baltas, M.; Gorrichon, L. *J. Org. Chem.* **2005**, *70*, 6921–6924.

(3) Najjar, F.; Gorrichon, L.; Baltas, M.; Vial, H.; Tzedakis, T.; André-Barrès, C. *Bioorg. Med. Chem. Lett.* **2003**, *14*, 1433–1436.

(4) Najjar, F.; André-Barrès, C.; Baltas, M.; Lacaze-Dufaure, C.; Magri, D. C.; Workentin, M. S.; Tzedakis, T. *Chem. Eur. J.* **2007**, *13*, 1174.

(5) Lacaze-Dufaure, C.; Najjar, F.; André-Barrès, C. *J. Mol. Struct.: THEOCHEM* **2007**, *803*, 17.

(6) Meshnick, S. R. *Int. J. Parasitol.* **2002**, *32*, 1655–1660.

(7) Robert, A.; Benoit-Vical, F.; Meunier, B. *Coord. Chem. Rev.* **2005**, *249*, 1927–1936.

(8) O'Neill, P. M.; Posner, G. H. *J. Med. Chem.* **2004**, *47*, 2945–2964.

(9) Eckstein-Ludwig, U.; Webb, R. J.; A. van Goethem, I. D.; East, J. M.; Lee, A. G.; Kimura, M.; O'Neill, P. M.; Bray, P. G.; Ward, S. A.; Krishna, S. *Nature* **2003**, *424*, 957–961.

(10) Gu, J.; Chen, K.; Jiang, H.; Leszczynski, J. *J. Phys. Chem. A* **1999**, *103*, 9364.

(11) Taranto, A. G.; de M. Carneiro, J. W.; de Oliveira, F. G.; de Araujo, M. T.; Correa, C. R. *J. Mol. Struct.: THEOCHEM* **2002**, *580*, 207.

(12) Arantes, C.; de Araujo, M. T.; Taranto, A. G.; de M. Carneiro, J. W. *Int. J. Quantum Chem.* **2005**, *103*, 749.

(13) Drew, M. G. B.; Metcalfe, J.; Ismail, F. M. D. *J. Mol. Struct.: THEOCHEM* **2004**, *711*, 95.

(14) Drew, M. G. B.; Metcalfe, J.; Ismail, F. M. D. *J. Mol. Struct.: THEOCHEM* **2005**, *756*, 87.

(15) Moles, P.; Oliva, M.; Safont, V. S. *J. Phys. Chem. A* **2006**, *110*, 7144.

(16) Modelli, A.; Galasso, V. *J. Phys. Chem. A* **2007**, *111*, 7787.

(17) Nosoongnoen, W.; Pratuangdejkul, J.; Sathirakul, K.; Jacob, A.; Contin, M.; Loric, S.; Launay, J. M.; Manivet, P. *Phys. Chem. Chem. Phys.* **2008**, *10*, 5083.

(18) Taranto, A. G.; de M. Carneiro, J. W.; de Araujo, M. T. *Bioorg. Med. Chem.* **2006**, *14*, 1546.

(19) Donkers, R. L.; Workentin, M. S. *J. Phys. Chem. B* **1998**, *102*, 4061.

(20) Maran, F.; Wayner, D. D. M.; Workentin, M. S. *Adv. Phys. Org. Chem.* **2001**, *36*, 85.

(21) Donkers, R. L.; Workentin, M. S. *Chem.—Eur. J.* **2001**, *7*, 4012.

(22) Antonello, S.; Maran, F. *J. Am. Chem. Soc.* **1999**, *121*, 9668.

(23) Antonello, S.; Formaggio, F.; Moretto, A.; Toniolo, C.; Maran, F. *J. Am. Chem. Soc.* **2001**, *123*, 9577.

(24) Marcus, R. A. *Biochim. Biophys. Acta* **1985**, *811*, 265.

(25) Rosso, K. M.; Dupuis, M. *J. Chem. Phys.* **2004**, *120*, 7050.

(26) Rosso, K. M.; Dupuis, M. *Theor. Chem. Acc.* **2005**, *116*, 124.

(27) Uudsemaa, M.; Tamm, T. *J. Phys. Chem.* **2003**, *107*, 9997.

(28) Hartnig, C.; Koper, M. T. M. *J. Am. Chem. Soc.* **2003**, *125*, 9840.

(29) Blumberger, J.; Sprik, M. *J. Phys. Chem. B* **2004**, *108*, 6529.

(30) Blumberger, J.; Sprik, M. *J. Phys. Chem. B* **2005**, *109*, 6793.

(31) Zeng, X.; Hu, H.; Hu, X.; Cohen, A. J.; Yang, W. *J. Chem. Phys.* **2008**, *128*, 124510.

(32) Marcus, R. A. *J. Chem. Phys.* **1956**, *24*, 966.

(33) Savéant, J. M. *Advances in Electron Transfer Chemistry*; JAI Press Inc.: Greenwich, CT, 1994; Vol. 4, p 53.

(34) Moens, J.; Geerlings, P.; Roos, G. *Chem. Eur. J.* **2007**, *13*, 8174.

(35) Frisch, M. J.; Trucks, G. W.; Schlegel, H. B.; Scuseria, G. E.; Robb, M. A.; Cheeseman, J. R.; Montgomery, J. A.; Vreven, J. T.; Kudin, K. N.; Burant, J. C.; Millam, J. M.; Iyengar, S. S.; Tomasi, J.; Barone, V.; Mennucci, B.; Cossi, M.; Scalmani, G.; Rega N.; Petersson, G. A.; Nakatsuji, H.; Hada, M.; Ehara, M.; Toyota, K.; Fukuda, R.; Hasegawa J.; Ishida, M.; Nakajima, T.; Honda, Y.; Kitao, O.; Nakai, H.; Klene, M.; Li, X.; Knox, J. E.; Hratchian, H. P.; Cross, J. B.; Adamo, C.; Jaramillo, J.; Gomperts, R.; Stratmann, R. E.; Yazyev, O.; Austin, A. J.; Cammi, R.; Pomelli, C.; Ochterski, J. W.; Ayala, P. Y.; Morokuma, K.; Voth, G. A.; Salvador, P.; Dannenberg, J. J.; Zakrzewski, V. G.; Dapprich, S.; Daniels, A. D.; Strain, M. C.; Farkas, O.; Malick, D. K.; Rabuck, A. D.; Raghavachari, K.; Foresman, J. B.; Ortiz, J. V.; Cui, Q.; Baboul, A. G.; Clifford, S.; Cioslowski, J.; Stefanov, B. B.; Liu, G.; Liashenko, A.; Piskorz, P.; Komaromi, I.; Martin, R. L.; Fox, D. J.; Keith, T.; Al-Laham, M. A.; Peng, C. Y.; Nanayakkara, A.; Challacombe, M.; Gill, P. M. W.; Johnson, B.; Chen, W.; Wong, M. W.; Gonzalez, C.; Pople, J. A. *Gaussian 03*, revision B.05; Gaussian, Inc.: Pittsburgh, PA, 2003.

(36) Becke, A. D. *J. Chem. Phys.* **1993**, *98*, 5648.

(37) Lee, C.; Yang, W.; Parr, R. G. *Phys. Rev. B* **1988**, *37*, 785.

(38) Sterns, M. *J. Cryst. Mol. Struct.* **1971**, *1*, 373.

(39) Parr, R. G.; Yang, W. *Density Functional Theory of Atoms and Molecules*; Oxford University Press: Oxford, U.K., 1989; p 276.

(40) Parr, R. G.; Szentpaly, L. V.; Liu, S. *J. Am. Chem. Soc.* **1999**, *121*, 1922.

(41) Chattaraj, P. K.; Sarkar, U.; Roy, D. R. *Chem. Rev.* **2006**, *106*, 2065.

(42) (a) Savéant, J.-M. In *Advances in Electron Transfer Chemistry*; Mariano, P. S., Ed.; JAI Press Inc.: Greenwich, CT, 1994; Vol. 4, p 53. (b) Savéant, J.-M. In *Advances in Physical Organic Chemistry*; Tidwel, T., Ed.; Academic Press: New York, 2000; Vol. 35, p 117.

(43) Magri, D. C.; Donkers, R. L.; Workentin, M. S. *J. Photochem. Photobiol., A* **2001**, *138*, 29.

JP100718P